THE JOURNAL OF PHYSICAL CHEMISTRY C
A JOURNAL OF THE AMERICAN CHEMICAL SOCIETY

pubs.acs.org/JPCC

Article

Controlled CVD Growth of Highly ⟨111⟩-Oriented 3C-SiC

Jing-Jia Huang, Christian Militzer, Charles Wijayawardhana, Urban Forsberg, Lars Ojamäe, and Henrik Pedersen*

Cite This: *J. Phys. Chem. C* 2022, 126, 9918–9925

Read Online

ACCESS | Metrics & More | Article Recommendations

ABSTRACT: Highly ⟨111⟩-oriented 3C-SiC coatings with a distinct surface morphology consisting of hexagonally shaped pyramidal crystals were prepared by chemical vapor deposition (CVD) using silicon tetrachloride ($SiCl_4$) and toluene (C_7H_8) at $T \leq 1250$ °C and $p_{tot} = 10$ kPa. In contrast, similar deposition conditions, with methane (CH_4) as the carbon precursor, resulted in randomly oriented 3C-SiC coatings with a cauliflower-like surface of SiC crystallites. No excess carbon was detected in the highly ⟨111⟩-oriented 3C-SiC samples despite the use of aromatic hydrocarbons. The difference in the preferred growth orientation of the 3C-SiC coatings deposited by using C_7H_8 and CH_4 as the carbon precursors was explained via quantum chemical calculations of binding energies on various crystal planes. The adsorption energy of C_6H_6 on the SiC (111) plane was 6 times higher than that on the (110) plane. On the other hand, CH_3 exhibited equally strong adsorption on both planes. This suggested that the highly ⟨111⟩-oriented 3C-SiC growth with C_7H_8 as the carbon precursor, where both C_6H_6 and CH_3 were considered the main active carbon-containing film forming species, was due to the highly preferred adsorption on the (111) plane, while the lower surface energy of the (110) plane controlled the growth orientation in the CH_4 process, in which only CH_3 contributed to the film deposition.

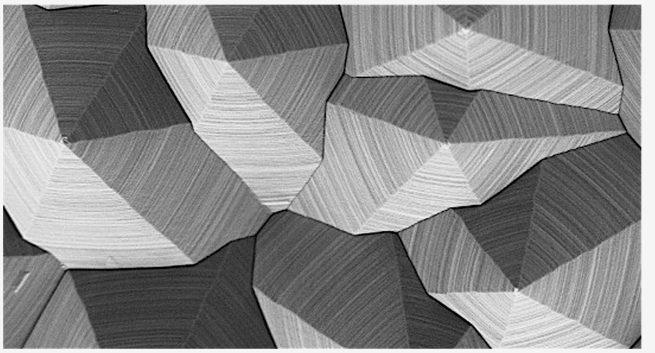

INTRODUCTION

Polycrystalline silicon carbide (SiC) is a protective coating of choice in many industries due to its high chemical inertness, hardness, and temperature stability. Among the SiC polytypes, cubic SiC, also known as 3C- or β-SiC, is the most used in refractory applications due to its relatively low formation temperature. One of the techniques frequently adopted for the synthesis of polycrystalline 3C-SiC is chemical vapor deposition (CVD).[1] In a SiC CVD process, multicomponent precursors, e.g., methyltrichlorosilane, can ensure unity of the C/Si ratio in the gas phase, whereas single-component precursors containing only C or Si can grant the process extra degrees of freedom in choosing different silicon and carbon precursors.[2] Chlorinated silanes, especially silicon tetrachloride ($SiCl_4$), are widely used silicon precursors in many SiC processes. The addition of Cl to the SiC CVD processes has been reported to not only increase the growth rate but also prevent the formation of Si droplets in the gas phase. The stronger Si−Cl bonds (400 kJ/mol)[3] can suppress the formation of weaker Si−Si bonds (226 kJ/mol).[3,4] In terms of the carbon precursor, small hydrocarbons such as ethylene or propane are often used because they can produce high-quality SiC coatings and are available at high purities.

As in many polycrystalline materials, the physical and chemical properties of 3C-SiC coatings are dependent on the crystalline orientation. It has been shown that the Vickers microhardness of ⟨111⟩-oriented 3C-SiC films, i.e., films in which the (111) planes were aligned parallel to the surface, was higher than those that were ⟨110⟩-oriented.[5] The (110) and (111) planes are the two planes in 3C-SiC with the lowest surface energy, 3.4 and 4.2 J/m^2, respectively.[6] In the $SiCl_4$-based 3C-SiC CVD processes, the preferred growth orientation of resultant coatings varies with the selection of hydrocarbons as well as the deposition conditions. It was reported that by use of CH_4 as the carbon precursor, highly ⟨111⟩-oriented 3C-SiC could be produced either at $T = 1200$ °C, $p_{tot} = 4$ kPa[7] or at $1200 < T \leq 1500$ °C, $p_{tot} \geq 40$ kPa.[8] On the other hand, at $T = 1450$ °C, $p_{tot} = 1$ kPa or at $T > 1450$ °C, $p_{tot} \leq 10$ kPa, highly ⟨110⟩-oriented 3C-SiC was obtained.[8] Similarly, with C_3H_8 as carbon precursor, the growth at $T = 1200$ °C, $p_{tot} = 4$ kPa, was highly ⟨111⟩-oriented but switched to ⟨110⟩ at elevated temperatures.[7,9] No explanation for these changes in preferred growth orientation was suggested in these studies. Highly

Received: February 17, 2022
Revised: May 17, 2022
Published: June 4, 2022

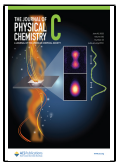

https://doi.org/10.1021/acs.jpcc.2c01171
J. Phys. Chem. C 2022, 126, 9918–9925

⟨111⟩-oriented 3C-SiC has also been prepared with hexamethyldisilane via laser CVD.[10−14] However, because of the small laser spot size, the coating area was limited to less than 20 × 20 mm^2.

Although it appears that small aliphatic hydrocarbons are favored in the 3C-SiC CVD, presumably because of their relatively simpler structures, the use of aromatics as the carbon precursor in CVD of other metal carbides has been reported. Nagai et al. deposited β-Mo_2C thin films using benzene as the carbon precursor,[15] whereas toluene was used for the deposition of SiC reported by Zhuravlov et al.[16] TiC_x was prepared from both benzene[17] and toluene.[18] However, either amorphous carbon or pyrolytic graphite was detected in most of these carbide films. Despite the risk of carbon codeposition, the use of aromatic hydrocarbons as the carbon precursor may also influence the preferred growth orientation of deposited films. In the work of Leonhardt et al., a transition of preferred growth orientation from ⟨100⟩ to ⟨111⟩ with the change of carbon precursor from aliphatic, e.g., methane, to aromatic hydrocarbons, e.g., benzene, was observed in the growth of TiC_x. This phenomenon was later interpreted by Pedersen et al. through quantum chemical calculations where they claimed that the adsorption energy of benzene molecules on TiC(111) planes was higher than that on TiC(100), resulting in a ⟨111⟩-oriented growth, whereas methane molecules did not exhibit preferential adsorption on either planes, and therefore TiC would preferentially grow on the plane that has the lowest surface energy, i.e., (100) in TiC.[19] While both TiC and 3C-SiC are face-centered-cubic crystal systems, TiC adopts the rock-salt structure (B1,[20] No. 225[21]) and 3C-SiC the zincblende structure (B3,[20] No. 216[21]). Despite their structural difference, the crystal plane along the ⟨111⟩ direction in both crystals is terminated only with either C or Si/Ti atoms. This indicates that the (111) planes of TiC and 3C-SiC may exhibit similar properties for adsorbing molecules; therefore, the growth direction of 3C-SiC can possibly be steered in the same way as in the growth of TiC.

In this work, we test this hypothesis and demonstrate the possibility of controlling the preferred growth orientation of polycrystalline 3C-SiC between ⟨111⟩ and ⟨110⟩ by using either toluene or methane as the carbon precursors in the $SiCl_4$-based SiC CVD. Furthermore, by quantum chemical calculations, we show how the adsorption behavior of benzene and methyl group differs when they approach the 3C-SiC (111) and (110) planes.

METHODS

Film Deposition. 3C-SiC coatings were deposited on isostatic graphite substrates (100 mm × 60 mm × 1.5 mm) via a horizontal hot-wall CVD reactor by using silicon tetrachloride ($SiCl_4$) and either methane (CH_4) or toluene (C_7H_8). Liquid $SiCl_4$ and C_7H_8 were stored in the stainless-steel bubblers placed in a water bath whose temperature was maintained at 24.3 °C by a thermostat. The corresponding vapor pressure of $SiCl_4$ and C_7H_8 at this temperature was 30.7 and 3.6 kPa, respectively. Hydrogen, purified by Ag−Pd alloy membranes, was utilized as both a reacting and carrier gas, directing the precursors from the bubblers to the reaction chamber. During the deposition, the substrate was situated in an inductively heated SiC-coated graphite susceptor. The temperature control within the reactor was realized by an optical pyrometer which measured the temperature through a view port. A throttle valve located between the chamber and the process pump regulated the pressure by adjusting its degree of opening. All 3C-SiC coatings in this study were prepared at a total pressure of 10 kPa with a p_C/p_{Si} = 1 and a p_{H_2}/p_{Si} = 23 in the gas phase, at temperatures between 1100 and 1350 °C for the C_7H_8 process and between 1100 and 1400 °C for the CH_4 process.

Characterization. The 3C-SiC-coated graphite plates were broken into four equal-sized pieces along the gas flow direction to probe the film deposition. The characterizations, i.e., X-ray diffraction (XRD), scanning electron microscopy (SEM), and Raman measurement, were performed mainly on the third piece counting from the inlet of the susceptor. The chemical phase of the as-deposited samples was examined by XRD (PANalytical X'Pert PRO powder X-ray diffractometer) operating at a voltage of 45 kV and a current of 40 mA. The characteristic Cu Kα radiation with a wavelength of 1.54 Å was used to perform the $\theta/2\theta$-scan between 20° and 140° in a Bragg−Brentano configuration with a divergence and an antiscatter slit of 0.5°. A Ni filter was placed before the X'Celerator detector running in scanning line mode to remove the Cu Kβ line. The resultant diffraction patterns were compared to the Powder Diffraction File (PDF) cards, and the reflection peaks corresponding to certain lattice planes were assigned. The PDF cards referenced for 3C-SiC and graphite in this work were #00-029-1129 and #00-056-0159, respectively. The preferred growth orientation of the 3C-SiC coatings was quantified by the texture coefficient (TC)[9] defined as follows:

$$\mathrm{TC}_{(hkl)} = \frac{I_{m(hkl)}/I_{0(hkl)}}{\left(\frac{1}{n}\right)\sum [I_{m(hkl)}/I_{0(hkl)}]}$$

where (hkl) is the growth plane considered, I_m the normalized measured intensity (with the background intensity subtracted), I_0 the intensity of a randomly oriented polycrystalline sample (taken from the PDF card), and n the number of planes that are considered. Here, planes (111), (200), (220), (311), (222), and (331) were used for the TC calculation; therefore, n was equal to 6. The surface morphology and the cross section of the samples were probed by a field emission SEM (ZEISS LEO1550) using an acceleration voltage of 3 kV at a working distance around 5 mm. The existence of pyrolytic carbon in the coatings was investigated by a Raman spectrometer where an Ar laser with a wavelength of 532 nm and a power of 10 mW was employed to excite the chemical bonds.

Computational Methods. The adsorption behaviors of C_6H_6 and CH_3 species on 3C-SiC (111) and (110) planes were studied by quantum chemical calculation via the software Gaussian 16.[22] The (111) and (110) planes were modeled by using $Si_{15}C_{15}$ and $Si_{16}C_{16}$ clusters, respectively, both containing four atomic planes. To preserve the bulk structure of SiC, the lateral and the bottom side of the clusters were saturated with hydrogen atoms. As for the top surface, the (111) plane was terminated with Si atoms without H-saturation, while on the (110) plane only C atoms were saturated with hydrogen. The geometries of these clusters were optimized by calculations based on density functional theory (DFT) using B3LYP functionals[23,24] with the 6-31G(d,p) basis set and the empirical dispersion corrections D3 proposed by Grimme et al.[25] The spin configuration giving the lowest energy and the least distorted structure were used for each cluster. The adsorption energy, E_{ads}, was calculated as follows:

$$E_{ads} = E_{\text{optimized geometry}} - (E_{\text{cluster}} + E_{\text{molecule}})$$

https://doi.org/10.1021/acs.jpcc.2c01171
J. Phys. Chem. C 2022, 126, 9918−9925

where $E_{cluster}$ and $E_{molecue}$ are the energy of bare surfaces and of species, e.g., C_6H_6 or CH_3, in the gas phase, respectively, while $E_{optimized\ geometry}$ is the energy of the optimized structure including both adsorbate and adsorbent.

RESULTS AND DISCUSSION

The use of C_7H_8 as carbon precursor resulted in distinct surface morphologies and cross sections as shown in Figures 1

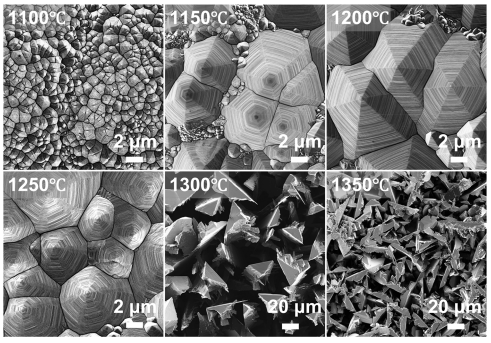

Figure 1. Surface morphologies of 3C-SiC coatings deposited with $SiCl_4$ and C_7H_8 at various temperatures.

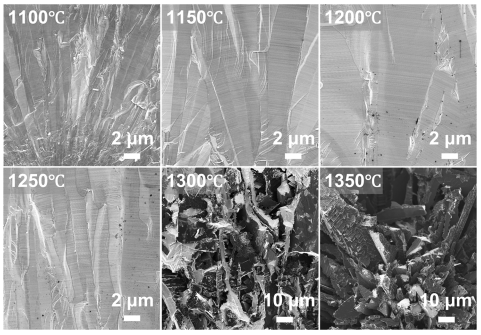

Figure 2. Cross sections of 3C-SiC coatings deposited with $SiCl_4$ and C_7H_8 at various temperatures.

and 2, respectively. At a deposition temperature equal to or lower than 1250 °C, the growth is columnar, and the sample surface is dominated with the crystals resembling the top of hexagonal pyramids. It can also be noticed that the crystal size first increases when temperature rises from 1100 to 1200 °C and slightly decreases at 1250 °C. The 6-fold symmetric pyramids are assumed to be formed by a pair of twin triangular pyramids joining each other[12] and are a typical morphology of coatings with ⟨111⟩-oriented face-centered-cubic (FCC) crystal structure,[26] whereas the pyramids with 4-fold symmetry were reported to be FCC crystals with ⟨110⟩ orientation.[26] The dense and dark striations seen in either the surface morphologies (Figure 1) or the cross sections (Figure 2) of the samples prepared at $T \leq 1250$ °C have previously been shown to be twins parallel to the (111) planes,[13] implying that these samples are highly ⟨111⟩-oriented. When the temperature is further increased above 1300 °C, the surface turns into loose fibers and the coating becomes porous, suggesting a different deposition chemistry.

Figure 3a presents the θ–2θ scan X-ray diffractograms of the coatings prepared with $SiCl_4$ and C_7H_8 at various temperatures. 3C-SiC is the major crystalline phase detected in most

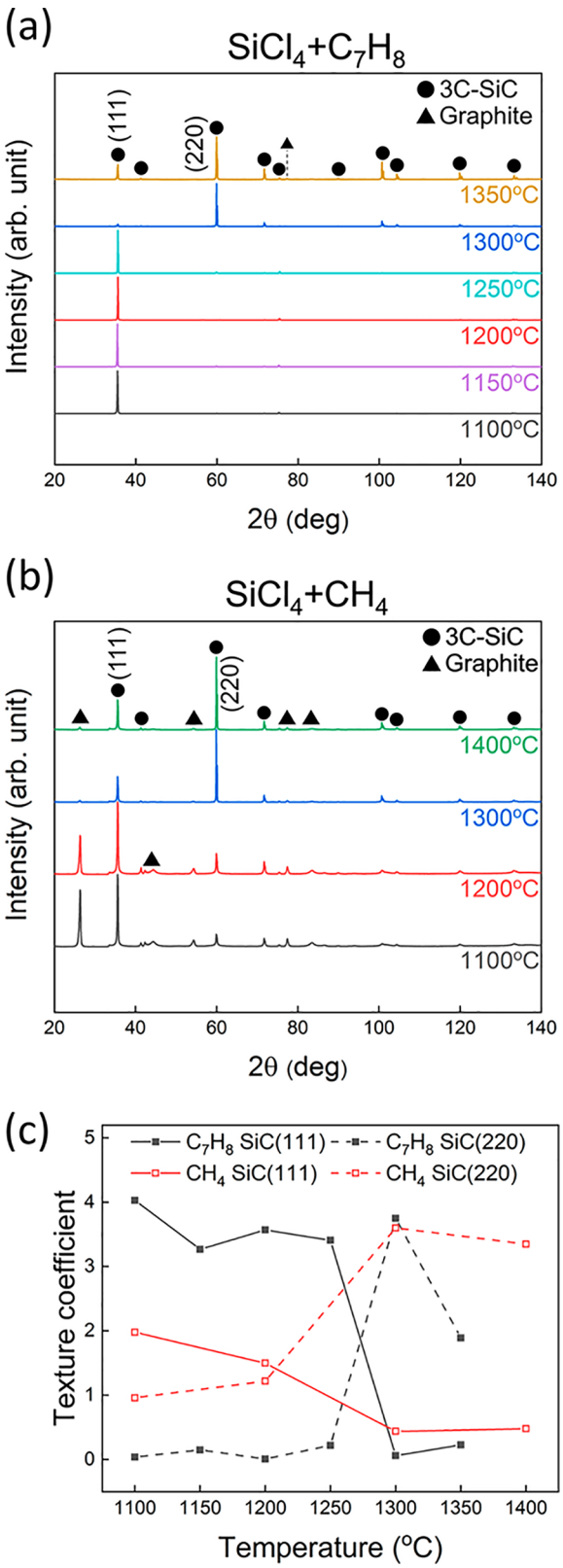

Figure 3. X-ray θ–2θ scan diffractograms of 3C-SiC coatings deposited at various temperatures with (a) C_7H_8 and (b) CH_4 as the carbon precursor. (c) Variation of (111) and (220) texture coefficients with the deposition temperatures.

of the samples. At $T \leq 1250$ °C, the samples are highly ⟨111⟩-oriented because the diffractions from 3C-SiC (111), (222), and (333) planes, corresponding to the 2θ of 35.6°, 75.5°, and

https://doi.org/10.1021/acs.jpcc.2c01171
J. Phys. Chem. C 2022, 126, 9918−9925

133.4°, are almost the only peaks observed. At $T \geq 1300$ °C, the intense peak from 3C-SiC (220) plane at $2\theta = 60.0°$ indicates that the coatings are more ⟨110⟩-oriented. At $T = 1350$ °C, a rather weak graphite peak at $2\theta = 77.5°$ from the substrate is also observed.

Under similar conditions, CH_4 was also utilized for the growth of 3C-SiC coatings. The surface morphologies, cross sections, and diffractograms of the deposited coatings are displayed in Figures 4, 5, and 3b, respectively. At $T \leq 1200$ °C,

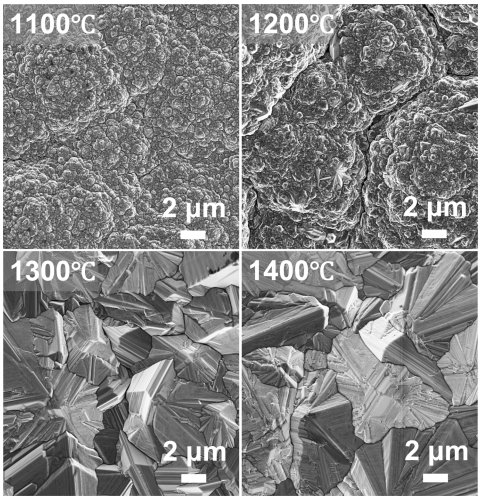

Figure 4. Surface morphologies of 3C-SiC coatings deposited with $SiCl_4$ and CH_4 at various temperatures.

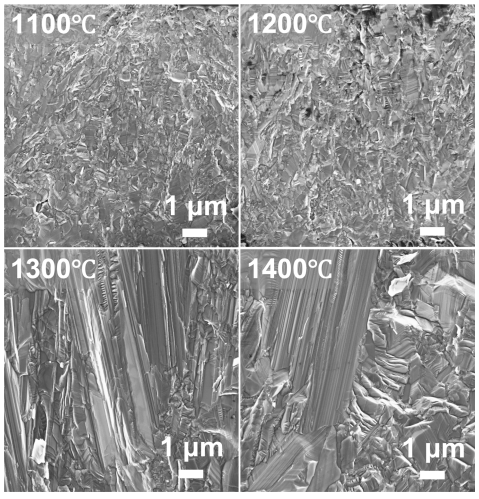

Figure 5. Cross sections of 3C-SiC coatings deposited with $SiCl_4$ and CH_4 at various temperatures.

the surface resembles cauliflowers with small, nonfaceted SiC crystallites, whereas at $T > 1200$ °C the faceted crystals which increase in size with increasing deposition temperature are formed. A growth mode transition from fine crystallite to columnar with increasing temperature can be observed in the cross-sectional images shown in Figure 5. In contrast to the C_7H_8 process where a shift of growth orientation from ⟨111⟩ to ⟨110⟩ was seen with higher temperatures, the diffractograms for the 3C-SiC coatings prepared in the CH_4 process show a change from randomly oriented to ⟨110⟩-oriented growth between 1200 and 1300 °C.

In Figure 3c the quantified growth orientation, i.e., the texture coefficient (TC), of the 3C-SiC coatings deposited with C_7H_8 and CH_4 is plotted versus the deposition temperature. The (111) and (110) planes of 3C-SiC are chosen for comparison because they are the first and second strongest reflections in the diffractogram of the randomly oriented polycrystalline 3C-SiC powder. For both C_7H_8 and CH_4 processes, a transition of growth orientation can be observed. At higher temperatures (C_7H_8: $T \geq 1300$ °C; CH_4: $T > 1200$ °C), the 3C-SiC coatings from both processes are highly ⟨110⟩-oriented. At lower temperatures (C_7H_8: $T \leq 1250$ °C; CH_4: $T < 1200$ °C), the 3C-SiC coatings deposited with CH_4 exhibit no strongly preferred growth orientation, whereas the ones prepared with C_7H_8 are highly ⟨111⟩-oriented. These observations are in accord with the change of the surface morphology seen in the SEM images. Because the deposition conditions in both sets of experiments were similar except for the used hydrocarbon, it is inferred that the difference in growth orientation at low temperature is caused by the choice of hydrocarbon.

To investigate whether the use of aromatic hydrocarbons would result in the formation of excess carbon in the films, the Raman measurements were performed on the 3C-SiC coatings deposited with either CH_4 or C_7H_8 as shown in Figure 6. In the CH_4 process, the Raman spectra of the deposited 3C-SiC coatings show a Raman shift deviation of ± 1 cm^{-1} in both first order 3C-SiC transverse optical (TO) and longitudinal optical (LO) mode. The Raman shifts for first-order TO and MO modes of bulk 3C-SiC were reported to be 796 and 972 cm^{-1}, respectively.[27] On the other hand, an even higher deviation of Raman shift for first-order TO and MO modes is observed in the 3C-SiC coatings prepared with C_7H_8 with the corresponding TO at 794 ± 2 cm^{-1} and LO at 967 ± 2 cm^{-1}. The second-order TO and LO modes of 3C-SiC[28] at 1520 and 1710 cm^{-1}, respectively, are also detected in both processes. Moreover, at lower temperatures (C_7H_8: $T < 1200$ °C; CH_4: $T \leq 1200$ °C), broadened transverse acoustic (TA) and longitudinal acoustic (LA) modes of 3C-SiC, which are normally located between 150 and 600 cm^{-1}, are observed, indicating the existence of smaller SiC crystallites.[29−31] However, at $T \geq 1300$ °C, the characteristic Raman modes for carbon phases, e.g., D-band at 1350 cm^{-1}, G-band at 1580 cm^{-1}, and 2D band at 2701 cm^{-1},[29] are observed in the 3C-SiC samples prepared with C_7H_8, indicating the codeposition of the pyrolytic carbon. It is noteworthy that the appearance of these Raman peaks is observed at the same temperature as the shift from ⟨111⟩- to ⟨110⟩-oriented growth. This could be caused by the breakdown of the toluene molecules, which forms highly reactive intermediates at such high temperatures. It could also be possible that the Si precursor is depleted faster than the C precursor, leaving excess carbon species in the coating. Either way, the presence of pyrolytic carbon indicates a change in the growth chemistry, which could be the cause of the change in crystalline orientation and morphology as seen in SEM and XRD. Interestingly, no signs of pyrolytic carbon can be found in the coatings grown from CH_4, even at high temperatures. A possible explanation is the different decomposition products of the hydrocarbons. Toluene will decompose into larger hydrocarbons that may more easily form condensed deposits, while CH_4 will only break down into even smaller radicals, which are less prone to form condensed pyrolytic carbon deposits.

https://doi.org/10.1021/acs.jpcc.2c01171
J. Phys. Chem. C 2022, 126, 9918−9925

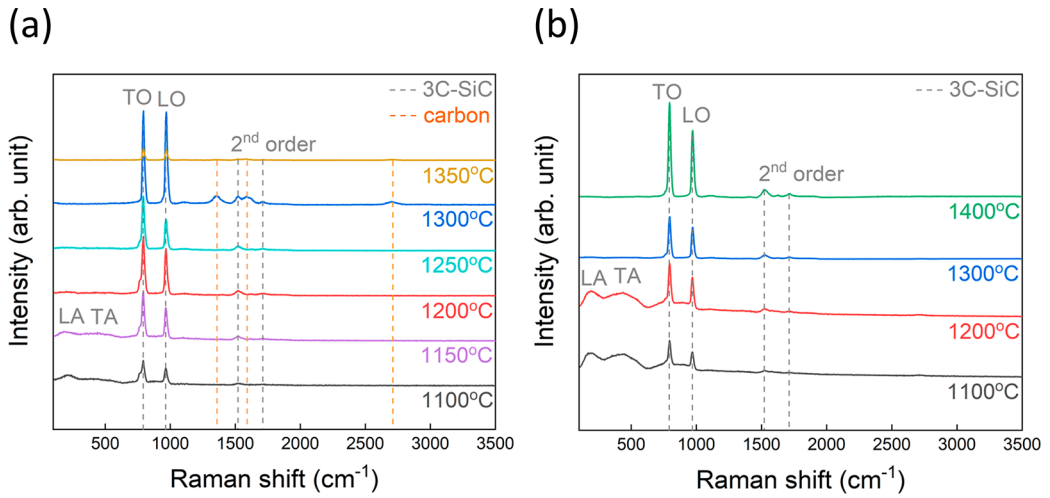

Figure 6. Raman spectra of 3C-SiC coatings deposited at various temperatures with $SiCl_4$ as the Si precursor and (a) C_7H_8 and (b) CH_4 as the carbon precursor.

The different growth regimes in the C_7H_8 process can also be observed in the Arrhenius plot displayed in Figure 7, where

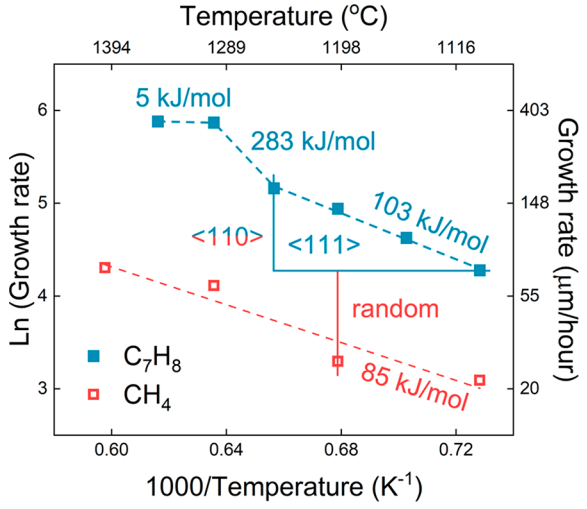

Figure 7. Arrhenius plot for the $SiCl_4$-based 3C-SiC coatings with either CH_4 or C_7H_8 as the carbon precursor. The data points from both processes are fitted with dashed lines.

the reciprocal temperature is plotted versus natural logarithm of the growth rate instead of the rate constant, as is the case in much literature on CVD coatings.[1] From the data, there seems to be three growth regimes in the C_7H_8 process. For $T \leq 1250$ °C, the Arrhenius plot suggests that the growth is kinetically limited with an activation energy of 103 kJ/mol. At 1250 °C < T < 1300 °C, the kinetics-controlled growth seems to retain but with a much higher activation energy. In this temperature range, the preferred growth orientation of 3C-SiC deposited with toluene switches from the ⟨111⟩ to ⟨110⟩ direction, and free carbon also starts to be incorporated into the films. The change of the slope in the Arrhenius plot and in the preferred growth orientation can be interpreted as an indication of change in the deposition chemistry. It should be noted that a change in deposition chemistry can also result in a change in the reaction order of the rate-determining step, meaning that for example the rate constant in the Arrhenius equation is not the same over the entire investigated temperature range in Figure. 7. When the temperature continues to rise above 1300 °C, the deposition again alters its character, and the films grow in the form of more flakelike crystals (Figure 1). This alteration is represented by a plateau in Figure 7, suggesting that at $T \geq$ 1300 °C the deposition chemistry enters the mass-transport-limited regime with an apparent activation energy of 5 kJ/mol. On the other hand, the 3C-SiC growth in the CH_4 process appears to be kinetics limited with an activation energy of 85 kJ/mol between 1100 and 1400 °C, and the preferred growth orientation changes from randomly oriented to highly ⟨110⟩ at T > 1200 °C.

To further understand the deposition chemistry, the adsorption behaviors of C_6H_6 and CH_3 on the 3C-SiC (111) and (110) planes were studied by DFT calculations. A toluene molecule consists of a benzene ring (C_6H_6) with one of its H atoms replaced by a methyl group (CH_3) and was reported to undergo two possible decomposition pathways:[32,33]

$$H_2 + C_6H_5CH_3 \rightarrow C_6H_6 + CH_4 \quad (1)$$

$$H + C_6H_5CH_3 \rightarrow C_6H_6 + CH_3 \quad (2)$$

Reaction 1 could occur already at 540 °C in a H_2 atmosphere,[32] while at higher temperatures reaction 2 was shown to be more prominent;[33] the CH_4 generated from reaction 1 could further react with H_2, forming CH_3 radicals. From a previous TiC CVD study,[17] using C_6H_6 as the carbon precursor resulted in ⟨111⟩-oriented TiC via thermal CVD and ⟨100⟩-oriented TiC by plasma-enhanced CVD. As the C_6H_6 molecule was expected to break down in the plasma, the results indicated that it survived at CVD temperatures. Considering a partial pressure ratio ($p_{H_2}/p_{C_7H_8}$) of 163 and a deposition temperature around 1200 °C, it can be assumed that C_6H_6 and CH_3 are the active carbon species in the C_7H_8 process. On the other hand, in the CH_4 process, because of the indirect contribution of CH_4 molecule toward the SiC growth,[34] CH_3 radicals from the decomposition of CH_4 are considered to be the only active carbon species. In this regard, C_6H_6 and CH_3 were chosen for the adsorption studies. Figure 8 presents the calculation results for the adsorption of the above-mentioned two species on 3C-SiC (111) and (110) planes. It can be noticed that CH_3 is easily adsorbed on both planes, and the adsorption energy on (111) and (110) is calculated to be −376 and −368 kJ/mol, respectively. Moreover, the distance

https://doi.org/10.1021/acs.jpcc.2c01171
J. Phys. Chem. C 2022, 126, 9918−9925

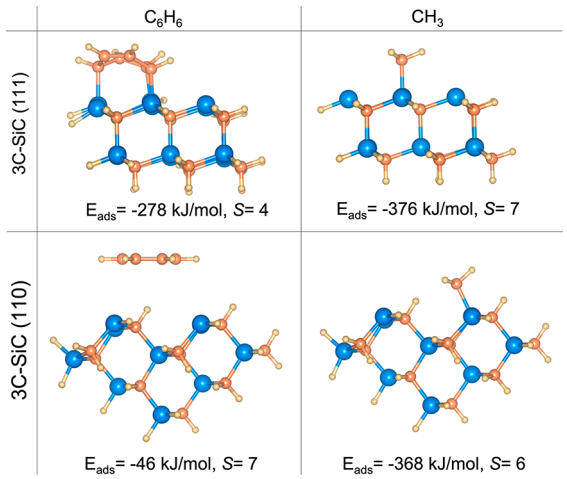

Figure 8. Computational results of the adsorption of C_6H_6 and CH_3 on 3C-SiC (111) and (110) planes and their corresponding adsorption energies, E_{ads}. S denotes the spin configuration that yielded the lowest energy and the least distorted structure after calculation.

between the C atom from the CH_3 and the surface Si atom was reduced from the initial 2 Å position to 1.89 Å [(111) plane] and 1.90 Å [(110) plane] after adsorption, which is comparable to the C−H bond length in bulk 3C-SiC. The result suggests that the CH_3 radical does not show a strong preference toward the (111) or (110) plane because the adsorption energies of the CH_3 radical on both planes are very close to each other. The C_6H_6 molecule is also active toward the (111) plane, exhibiting an adsorption energy of −278 kJ/mol. Upon adsorption, the C_6H_6 molecule loses its planar symmetry: three C atoms of the molecule move away from the (111) surface, and the other three move down toward the (111) surface. The distance between the three C atoms closest to the surface and the surface Si atoms decreases to 1.95 ± 0.01 Å. However, the C_6H_6 molecule seems to be rather inactive toward the (110) plane, the distance between which after calculation increases from 2 to 3.54 Å, corresponding to an adsorption energy of −46 kJ/mol. Judging from the adsorption energy and the distance between the adsorbate and the surface, the C_6H_6 molecule is considered physiosorbed on the (110) plane, whereas the adsorption of C_6H_6 on (111) as well as that of CH_3 on both (111) and (110) surfaces can be described as chemisorption which would lead to the formation of chemical bonding.

The SiC crystals in the films are expected to grow along the atomic direction whose corresponding atomic plane has the lowest surface energy. According to Kikuchi et al., the surface energy of the first three low index 3C-SiC planes, namely, (100), (111), and (110), is 6.8, 4.2, and 3.4 J/m^2, respectively.[6] This implies that in the conventional 3C-SiC CVD most of the coatings would grow preferentially along the ⟨110⟩ direction. When we used CH_4 at 1100−1400 °C, we observed a random or ⟨110⟩-preferred growth direction. By use of C_7H_8 as the carbon precursor instead, it was possible to deposit highly ⟨111⟩-oriented 3C-SiC coatings at $T \leq 1250$ °C. This change of preferred growth orientation with aromatic hydrocarbons was previously observed for the CVD growth of TiC hard coatings.[17] For TiC, this was suggested to be due to the stronger adsorption of C_6H_6 on the (111) plane compared to the (100) plane, which overcame the lower surface energy of the (100) surface.[19] Based on the reported CVD chemistry for toluene,[32,33] the active carbon-containing film-forming species in the C_7H_8 process were assumed to be C_6H_6 and CH_3, whereas in the CH_4 process CH_3 was supposed to be the active species.[35] As described above, the computational results showed that CH_3 was chemisorbed on both 3C-SiC (111) and (110) planes, and C_6H_6 was chemisorbed on the (111) plane but physiosorbed on the (110) plane. The slight difference in the adsorption energies of CH_3 on both (111) and (110) explains the almost randomly oriented SiC growth in the CH_4 process. On the other hand, the highly ⟨111⟩-oriented 3C-SiC coatings prepared by using C_7H_8 can be assumed to result from the significant adsorption energy difference of C_6H_6 on (111) and (110) planes. The energy decrease resulting from the adsorption of C_6H_6 on the (111) plane is 6 times larger than that on (110). At higher temperatures, toluene is expected to decompose into various hydrocarbons,[36] and therefore the growth of 3C-SiC is no longer directed toward the ⟨111⟩ direction. Without the directing effect of the aromatic hydrocarbon, the growth happens mainly on the (110) planes having the lowest surface energy, which is similar to the case in the CH_4 process.

CONCLUSION

In this work, we were able to control the preferred growth orientation of 3C-SiC by using either methane (CH_4) or toluene (C_7H_8) as the carbon precursor in a $SiCl_4$-based SiC CVD. At $T \leq 1250$ °C and $p_{tot} = 10$ kPa, the resulting 3C-SiC coatings were highly ⟨111⟩-oriented in the C_7H_8 process, whereas they were almost randomly oriented in the CH_4 process. At $T > 1250$ °C both processes resulted in highly ⟨110⟩-oriented 3C-SiC coatings. By considering C_6H_6 and CH_3 the main active carbon-containing film forming species, their adsorption behaviors on 3C-SiC (111) and (110) planes were shown via quantum chemical calculation to be significantly different: C_6H_6 was chemisorbed on the (111) plane, but physisorbed on the (110) plane, while CH_3 was chemisorbed strongly on both planes. These calculation results indicate that the difference in reactivity of the carbon precursor toward the various planes is the reason for the different growth orientations. At $T > 1250$ °C, the transition to highly ⟨110⟩-oriented growth in both processes can be explained by the fact that 3C-SiC would tend to grow along the direction leading to the lowest surface energy, i.e., (110) plane in 3C-SiC. The steering effect of toluene is no longer present at elevated temperatures because of its expected decomposition into smaller, nonaromatic hydrocarbons.

AUTHOR INFORMATION

Corresponding Author

Henrik Pedersen − *Department of Physics, Chemistry and Biology, Linköping University, SE-581 83 Linköping, Sweden;* orcid.org/0000-0002-7171-5383; Email: henrik.pedersen@liu.se

Authors

Jing-Jia Huang − *Department of Physics, Chemistry and Biology, Linköping University, SE-581 83 Linköping, Sweden; SGL Carbon GmbH, DE-53170 Bonn, Germany*

Christian Militzer − *Department of Physics, Chemistry and Biology, Linköping University, SE-581 83 Linköping, Sweden; SGL Carbon GmbH, DE-53170 Bonn, Germany*

https://doi.org/10.1021/acs.jpcc.2c01171
J. Phys. Chem. C 2022, 126, 9918−9925

Charles Wijayawardhana − *SGL Carbon GmbH, DE-53170 Bonn, Germany*
Urban Forsberg − *Department of Physics, Chemistry and Biology, Linköping University, SE-581 83 Linköping, Sweden*
Lars Ojamäe − *Department of Physics, Chemistry and Biology, Linköping University, SE-581 83 Linköping, Sweden;* orcid.org/0000-0002-5341-2637

Complete contact information is available at: https://pubs.acs.org/10.1021/acs.jpcc.2c01171

Notes

The authors declare the following competing financial interest(s): The authors have filed a patent application based on the results.

■ ACKNOWLEDGMENTS

The authors thank SGL CARBON GmbH for the financial support. L. Ojamäe acknowledges support from the Swedish Research Council (VR). Rickard Liljedahl is acknowledged for fruitful discussions and for the support in sample characterizations.

■ REFERENCES

(1) Choy, K. Chemical Vapour Deposition of Coatings. *Prog. Mater. Sci.* **2003**, *48* (2), 57−170.
(2) Pedersen, H.; Leone, S.; Kordina, O.; Henry, A.; Nishizawa, S.; Koshka, Y.; Janzén, E. Chloride-Based CVD Growth of Silicon Carbide for Electronic Applications. *Chem. Rev.* **2012**, *112* (4), 2434−2453.
(3) Aylward, G.; Findlay, T. *SI Chemical Data*, 4th ed.; John Wiely & Sons: 1999.
(4) Yazdanfar, M.; Danielsson, Ö.; Kordina, O.; Janzén, E.; Pedersen, H. Finding the Optimum Chloride-Based Chemistry for Chemical Vapor Deposition of SiC. *ECS J. Solid State Sci. Technol.* **2014**, *3* (10), P320−P323.
(5) Kim, H.-S.; Choi, D.-J. The Reactant Depletion Effect on Chemically Vapor Deposited SiC Films with Pressure and Gas Ambient. *Thin Solid Films* **1998**, *312* (1−2), 195−201.
(6) Kikuchi, H.; Kalia, R. K.; Nakano, A.; Vashishta, P.; Branicio, P. S.; Shimojo, F. Brittle Dynamic Fracture of Crystalline Cubic Silicon Carbide (3C-SiC) via Molecular Dynamics Simulation. *J. Appl. Phys.* **2005**, *98* (10), 103524.
(7) Tu, R.; Zheng, D. H.; Cheng, H.; Han, M. X.; Zhang, S.; Goto, T. Preparation of Ultra-Thick β-SiC Films Using Different Carbon Sources. *Materials Research Innovations* **2015**, *19* (sup10), S10-397−S10-402.
(8) Tu, R.; Zheng, D.; Sun, Q.; Han, M.; Zhang, S.; Hu, Z.; Goto, T.; Zhang, L. Ultra-Fast Fabrication of < 110>-Oriented β-SiC Wafers by Halide CVD. *J. Am. Ceram. Soc.* **2016**, *99* (1), 84−88.
(9) Lin, T. T.; Hon, M. H. The Growth Characteristics of Chemical Vapour-Deposited β-SiC on a Graphite Substrate by the $SiCl_4/C_3H_8/H_2$ System. *J. Mater. Sci.* **1995**, *30* (10), 2675−2681.
(10) Xu, Q.; Zhu, P.; Sun, Q.; Tu, R.; Zhang, S.; Yang, M.; Li, Q.; Shi, J.; Li, H.; Zhang, L.; et al. Fast Preparation of (111)-Oriented β-SiC Films without Carbon Formation by Laser Chemical Vapor Deposition from Hexamethyldisilane without H_2. *J. Am. Ceram. Soc.* **2018**, *101* (4), 1471−1478.
(11) Zhu, P. P.; Tu, R.; Zhang, S.; Han, M. X.; Xu, Q. F.; Sun, Q. Y.; Zhang, L. M.; Goto, T.; Yan, J. S.; Li, S. S. The Effect of Diluent Gases on the Growth of β-SiC Films by Laser CVD with HMDS. *Materials Research Innovations* **2015**, *19* (sup10), S10-403−S10-407.
(12) Zhang, S.; Xu, Q.; Sun, Q.; Zhu, P.; Tu, R.; Hu, Z.; Han, M.; Goto, T.; Zhang, L.; Yan, J.; et al. Effect of Pressure on Microstructure of < 111>-Oriented β-SiC Films: Research via Electron Backscatter Diffraction. *J. Am. Ceram. Soc.* **2015**, *98* (12), 3713−3718.
(13) Zhang, S.; Xu, Q.; Tu, R.; Goto, T.; Zhang, L. High-Speed Preparation of < 111>- and < 110>-Oriented β-SiC Films by Laser Chemical Vapor Deposition. *J. Am. Ceram. Soc.* **2014**, *97* (3), 952−958.
(14) Zhang, S.; Xu, Q.; Tu, R.; Goto, T.; Zhang, L. Growth Mechanism and Defects of -Oriented β-SiC Films Deposited by Laser Chemical Vapor Deposition. *J. Am. Ceram. Soc.* **2015**, *98* (1), 236−241.
(15) Nagai, M.; Shishikura, I.; Omi, S. Molybdenum Carbide Prepared by Chemical Vapor Deposition. *Jpn. J. Appl. Phys.* **2000**, *39* (Part 1, No. 7B), 4528−4531.
(16) Zhuravlov, A. Y.; Hovanskiy, N. A.; Khizhnyak, D. A.; Shirokov, B. M.; Semenov, N. A.; Shijan, A. V.; Strigunovskiy, S. V.; Yevsiukov, A. I.; Shevtsov, A. B.; Nazarenko, E. A.; et al. Obtaining Silicon Carbide via Chemical Vapor, Plasma-Chemical and Sublimation Methods. *Problems of Atomic Science and Technology* **2017**.
(17) Leonhardt, A.; Wolf, E. Influence of Different Hydrocarbons on the Structure of CVD- and PACVD-TiC_x Hard Layers. *Materials Science and Engineering: A* **1996**, *209* (1−2), 389−393.
(18) López-Romero, S.; Chávez-Ramírez, J. Synthesis of TiC Thin Films by CVD from Toluene and Titanium Tetrachloride with Nickel as Catalyst. *Matéria (Rio de Janeiro)* **2007**, *12* (3), 487−493.
(19) Pedersen, H.; Lin, C.-C.; Ojamäe, L. On the Change of Preferential Growth Orientation in Chemical Vapor Deposition of Titanium Carbide by Aromatic Hydrocarbon Precursors. *Journal of Vacuum Science & Technology A: Vacuum, Surfaces, and Films* **2013**, *31* (2), 021507.
(20) Barrett, C.; Massalski, T. B. *Structure of Metals*, 3rd ed.; International Series on Materials Science and Technology; Pergamon: 1987.
(21) Hahn, T. *International Tables for Crystallography*, 5th ed.; Springer: 2002; Vol. *A*.
(22) Frisch, M. J.; Trucks, G. W.; Schlegel, H. B.; Scuseria, G. E.; Robb, M. A.; Cheeseman, J. R.; Scalmani, G.; Barone, V.; Petersson, G. A.; Nakatsuji, H.; et al. *Gaussian 16*, Revision C.01; Gaussian, Inc.: Wallingford, CT, 2019.
(23) Becke, A. D. Density-functional Thermochemistry. III. The Role of Exact Exchange. *J. Chem. Phys.* **1993**, *98* (7), 5648−5652.
(24) Lee, C.; Yang, W.; Parr, R. G. Development of the Colle-Salvetti Correlation-Energy Formula into a Functional of the Electron Density. *Phys. Rev. B* **1988**, *37* (2), 785−789.
(25) Grimme, S.; Antony, J.; Ehrlich, S.; Krieg, H. A Consistent and Accurate Ab Initio Parametrization of Density Functional Dispersion Correction (DFT-D) for the 94 Elements H-Pu. *J. Chem. Phys.* **2010**, *132* (15), 154104.
(26) Tu, R.; Zheng, D.; Cheng, H.; Hu, M.; Zhang, S.; Han, M.; Goto, T.; Zhang, L. Effect of $CH_4/SiCl_4$ Ratio on the Composition and Microstructure of < 110>-Oriented β-SiC Bulks by Halide CVD. *J. Eur. Ceram. Soc.* **2017**, *37* (4), 1217−1223.
(27) Feldman, D. W.; Parker, J. H.; Choyke, W. J.; Patrick, L. Phonon Dispersion Curves by Raman Scattering in SiC, Polytypes 3C,4H,6H,15R, and 21R. *Phys. Rev.* **1968**, *173* (3), 787−793.
(28) Feng, Z. C.; Tin, C. C.; Hu, R.; Williams, J. Raman and Rutherford Backscattering Analyses of Cubic SiC Thin Films Grown on Si by Vertical Chemical Vapor Deposition. *Thin Solid Films* **1995**, *266* (1), 1−7.
(29) Dasgupta, A.; Klein, S.; Houben, L.; Carius, R.; Finger, F.; Luysberg, M. Microstructure of Highly Crystalline Silicon Carbide Thin Films Grown by HWCVD Technique. *Thin Solid Films* **2008**, *516* (5), 618−621.
(30) Dasgupta, A.; Huang, Y.; Houben, L.; Klein, S.; Finger, F.; Carius, R.; Luysberg, M. Effect of Filament and Substrate Temperatures on the Structural and Electrical Properties of SiC Thin Films Grown by the HWCVD Technique. *Thin Solid Films* **2008**, *516* (5), 622−625.
(31) Ward, Y.; Young, R. J.; Shatwell, R. A. *A Microstructural Study of Silicon Carbide Fibres through the Use of Raman Microscopy* **2001**, 12.

(32) Amano, A.; Tominaga, H.; Tokuhisa, H. Mechanism of Thermal Hydrogenolysis of Toluene. *Bull. Japan Petrol. Inst.* **1965**, *7*, 59−63.
(33) Amano, A.; Horie, O.; Hanh, N. H. Effect of Thermal Activation on the Reaction of Toluene with Hydrogen Atoms. *Int. J. Chem. Kinet.* **1976**, *8* (3), 321−339.
(34) Sukkaew, P.; Danielsson, Ö.; Kordina, O.; Janzén, E.; Ojamäe, L. Ab Initio Study of Growth Mechanism of 4H−SiC: Adsorption and Surface Reaction of C_2H_2, C_2H_4, CH_4, and CH_3. *J. Phys. Chem. C* **2017**, *121* (2), 1249−1256.
(35) Stenberg, P.; Danielsson, Ö.; Erdtman, E.; Sukkaew, P.; Ojamäe, L.; Janzén, E.; Pedersen, H. Matching Precursor Kinetics to Afford a More Robust CVD Chemistry: A Case Study of the C Chemistry for Silicon Carbide Using SiF_4 as Si Precursor. *J. Mater. Chem. C* **2017**, *5* (23), 5818−5823.
(36) Derudi, M.; Polino, D.; Cavallotti, C. Toluene and Benzyl Decomposition Mechanisms: Elementary Reactions and Kinetic Simulations. *Phys. Chem. Chem. Phys.* **2011**, *13* (48), 21308.

https://doi.org/10.1021/acs.jpcc.2c01171
J. Phys. Chem. C 2022, 126, 9918−9925